ELSEVIER

Catalysis Today 36 (1997) 243–254

CATALYSIS TODAY

Synthesis of methyl methacrylate by vapor phase condensation of formaldehyde with propionate derivatives

Makarand R. Gogate[a], James J. Spivey[a,*], Joseph R. Zoeller[b]

[a] *Research Triangle Institute, , Research Triangle Park, NC 27709-2194, USA*
[b] *Eastman Chemical Company, , Kingsport, TN 37662-5150, USA*

Abstract

The gas phase condensation of formaldehyde with propionic acid, propionic anhydride, and methyl propionate was studied over a series of V–Si–P catalysts of varying atomic ratios. Propionic anhydride gave the maximum yield of methacrylic acid (56%, based on formaldehyde fed to the reactor) at 300°C, 2 atm, 290 cc g^{-1} h^{-1} and a stoichiometric anhydride/formaldehyde ratio of 2:1. This yield was obtained for the optimum V–Si–P catalyst, which had an atomic ratio of 1:10:2.8. This is the highest yield reported to date for the heterogeneous catalytic condensation of propionic anhydride with formaldehyde. A parameter called the q-ratio has been defined to correlate condensation yields to catalyst acid–base properties. Higher q-ratios ($0<q<1$) correspond to a higher proportion of strong acid sites and are directly related to higher condensation yields. The long-term deactivation studies on the V–Si–P 1:10:2.8 catalyst at 300°C, 2 atm and 290 cc g^{-1} h^{-1} show that catalyst activity drops by nearly a factor of 20 over a 180-h period, and that 78% of the activity can be restored by a mild oxidative regeneration. The performance of a V–Si–P catalyst has been compared to a Ta/SiO_2 catalyst; Ta catalyst is more stable and has a higher on-stream life.

Keywords: Methyl methacrylate; Condensation; Formaldehyde; Ternary catalysts

1. Introduction

The condensation of propionate derivatives with formaldehyde provides a novel synthetsis route to produce α-,β-unsaturated acids. These α-,β-unsaturated acids, and their ester derivatives, are among the most widely used industrial intermediates. They are polymerized to form plastic sheeting for signs, coatings, adhesives, fibers and paints. One compound of particular interest is methyl methacrylate (MMA) which can, in principle, be made from the condensation of various propionates with formaldehyde, yielding methacrylic acid (MAA), and the subsequent esterification of this acid with methanol to yield MMA. Three propionates, propionic anhydride (PAA), propionic acid (PA) and methyl propionate (MP), have been considered in this study. While the condensation of PA with MP and formaldehyde to form MAA is a known art and has been widely studied [1–3], the condensation of PAA with formaldehyde using a heterogeneous catalyst has been reported only in Ref. [4]. The condensation of PAA (rather than PA or MP) has the advantage of producing one mole less of water, which can kinetically inhibit the reaction, degrade the product, and make separation of the

*Corresponding author. Tel.: (1-919) 541-8030; Fax: (1-919) 541-8000; e-mail: jjs@rti.org

PII S0920-5861(96)00241-6

Table 1
Chemical structures and abbreviations of various compounds

Compound	Structure	Abbreviation
Propionic anhydride	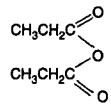	PAA
Propionic acid	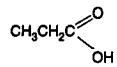	PA
Methyl propionate	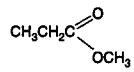	MP
Methacrylic acid	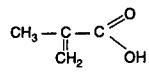	MAA
Methyl methacrylate	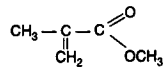	MMA
Diethyl ketone	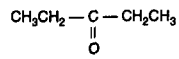	DEK
Formaldehyde		—
Methanol	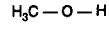	—

product more costly. The chemical structure and abbreviations of various components are summarized in Table 1.

The most widely practiced commercial technology for the synthesis of MAA and MMA is the acetone-cyanohydrin (ACH) process (Fig. 1). The ACH process requires handling of large quantities of extremely toxic and hazardous hydrogen cyanide (HCN) and generates copious amounts of ammonium sulfate wastes which are either discarded or reclaimed at a substantial cost.

The ACH technology is currently environmentally and economically untenable for any new expansions, primarily because of the cost of either disposing or regenerating the bisulfate waste.

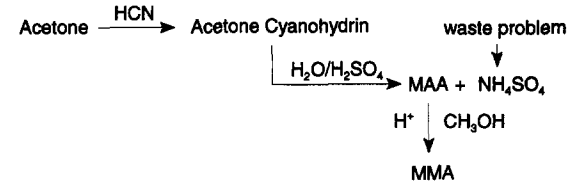

Fig. 1. Schematic of the ACH process.

There is a strong drive within the chemical industry for a replacement process [5,6]. In the United States, there is a particular interest in a process that is not petroleum-based, but is rather based on domestically produced coal-based syngas. The processes based on $C_2^=$-carbonylation shown in Fig. 2 are commercially attractive technologies for MMA manufacture [5,7]. Each of these four processes goes through a propionate intermediate, which is condensed with formaldehyde to produce either MAA (Processes (I) and (II)) or a mixture of MAA and MMA (Processes (III) and (IV)) (note that in Process (III), formaldehyde is produced by partial oxidation of methanol, which also esterifies the resulting MAA to MMA. The water produced in the partial oxidation reaction hydrolyzes a portion of the PAA to form PA, which is recycled). In Process (I), MAA is produced by the condensation of formaldehyde with propionaldehyde. The RTI–Eastman process (Process (III)) has the potential for a lower total cost, primarily because one less mole of water is produced. It comprises the following steps:

Step 1: Propionate synthesis from ethylene (Eq. (1)) *and ethylene plus PA* (Eq. (2))

$$H_2C{=}CH_2 + CO + H_2O \rightarrow CH_3CH_2COOH \quad (1)$$

$$CH_3CH_2COOH + CO + H_2C{=}CH_2 \rightarrow (CH_3CH_2CO)_2O \quad (2)$$

Step 2: Condensation of propionate with formaldehyde

$$(CH_3CH_2CO)_2O + HCHO \rightarrow CH_2{=}C(CH_3)COOH + CH_3CH_2COOH \quad (3)$$

$$CH_3CH_2COOH + HCHO \rightarrow CH_2{=}C(CH_3)COOH + H_2O \quad (4)$$

$$(CH_3CH_2CO)_2O + 2HCHO \rightarrow 2CH_2{=}C(CH_3)COOH + H_2O \quad (5)$$

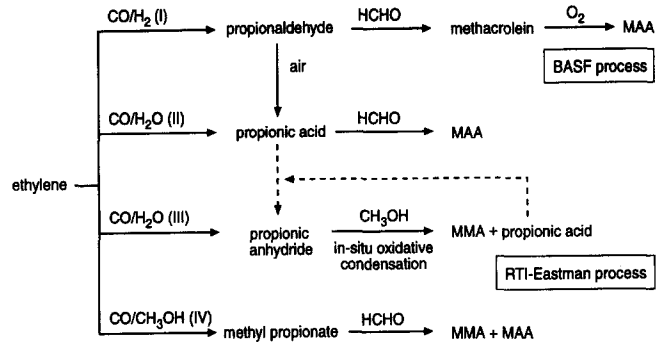

Fig. 2. C_2-carbonylation technologies for MMA manufacture.

Step 3: Esterification with methanol

$$CH_2{=}C(CH_3)COOH + CH_3OH \rightarrow CH_2{=}C(CH_3)COOCH_3 + H_2O \quad (6)$$

In this proposed process for MMA manufacture, Step 1 is commercially practiced by Eastman Chemical Company [5] and Step 3 is a known art. Step 2, however, presents a challenge for successful commercial demonstration of the process. This condensation step is composed of two separate condensation reactions ((3) and (4)) which give the overall stoichiometry shown in Reaction (5). Condensation of PA with formaldehyde (Reaction (4)) has been studied recently [1–3,8,9] using a V–Si–P catalyst which has both acid and base properties. However, these catalysts have not been tested for the condensation reaction of PAA and formaldehyde, and there are some obvious advantages to using the anhydride for the condensation reaction. For example, the condensation of formaldehyde with PA (Reaction (4)), and with MP and formaldehyde (Reaction (7)):

$$CH_3CH_2COOCH_3 + HCHO \rightarrow CH_2{=}C(CH_3)COOCH_3 + H_2O \quad (7)$$

yields 1 mol of water per mol MAA or MMA produced. This water inhibits the kinetics of this reaction and, in case of MP, also leads to hydrolysis of the ester (MP) itself. Water also complicates the downstream processing; hence it must be removed. However, when the condensation reaction is carried out using PAA (Reaction (5)), one mole less of water is produced (1 mol of water per 2 mol of MAA). In a stoichiometric excess of PAA, this water is consumed in a further reaction to produce PA:

$$(CH_3CH_2CO)_2O + H_2O \rightarrow 2CH_3CH_2COOH \quad (8)$$

This means that the overall condensation (Step 2) is carried out essentially anhydrously. There has been little reported on the gas phase condensation of formaldehyde and PAA, with only one reference available [4], in which a supported tantalum catalyst (10% Ta/SiO_2) was used for the condensation reaction. The work presented here compares the experimental results on the condensation of formaldehyde with each of the three propionates in Fig. 2 (PA, PAA and MP), and elucidates the effect of acid–base properties of the catalyst on the MAA yield.

2. Experimental

2.1. Catalyst preparation

The V–Si–P ternary catalysts were prepared with different ratios of the constituent atoms, following the procedure of Ai [1–3]. For example, V–Si–P catalyst with an atomic ratio of 1:12:2.8 was prepared as follows: 23.4 g NH_4VO_3 was dissolved in 100 ml hot water containing 20 ml lactic acid and 64.4 g of 85% H_3PO_4 were dissolved in 100 ml of hot water. The two solutions were added to 480 g of DuPont Ludox colloidal silica (Ludox SM-30), containing 30 wt% silica in water. Excess water was evaporated by stirring. The cake obtained was dried in an oven gradually heating from 50° to 200°C, at the rate of $1°C\ min^{-1}$. The resulting solid was crushed to an 8–20 mesh size portion and further calcined in air at 350°C for 4 h and then again at 450°C for 6 h.

The Ta catalysts were prepared using two different silica supports, namely a Davison G-59 silica support and a NALCO-1034A colloidal silica support, using conventional metal salt impregnation.

2.2. Catalyst testing

The V–Si–P and tantalum catalysts were tested in a continuous flow-type reaction apparatus. A nominally identical charge of 15, 10 and 5 g catalyst was used for comparative experiments. This corresponded to the space velocities of 290, 600 and 900 cc g^{-1} cat·h. The nominal flow rates of PAA, formaldehyde, and nitrogen were kept at 40, 20 and 220 mmol h^{-1}. The actual flow rates varied slightly, and exact values are reported in Section 3. For PA and MP feeds, the mole ratio of the propionyl to formaldehyde was approximately 4. The feed was prepared by dissolving 1,1,1-trioxane (a trimer of formaldehyde, solid at room temperature) into the substrate propionyl and feeding the mixture to a preheater using a syringe pump (ATI Orion SAGE M361). The vaporized feed was passed over the catalyst charge, located centrally in a 6 mm ID×356 mm L SS 316 reactor tube. The catalyst charge was held in place by glass wool and beads. Both the preheater and the reactor were mounted horizontally in a Lindberg furnace (Blue M, Model # TF55035A). A thermocouple mounted directly in the catalyst bed provided temperature control and readout. The product vapors were cooled in a water condenser. Permanent gases were analyzed on-line. Liquid products were analyzed off-line.

2.3. Product analysis

For gas analysis, a fixed-volume loop injection onto a Poropak® T/molecular sieve 5A and a column isolation sequence in conjunction with a thermal conductivity detector (TCD) were used. For liquid analysis, a fused silica capillary column with a 1 mm film thickness of DB-wax was used in conjunction with a flame ionization detector (FID).

2.4. Catalyst characterization

The catalysts were analyzed for their surface area, pore volume and acid–base properties. The surface area and pore volume determinations were made on a Qunatchrome NOVA 1000 BET-N_2 surface-area analyzer. The acid–base properties were determined using an ALTAMIRA AMI-100 catalyst characterization instrument. For measurement of acid sites and strength, NH_3–TPD was used. A 10% NH_3–N_2 gas mixture was used as the treatment or adsorbing gas. A nominally identical charge of 150 mg of catalyst sample was used for all measurements. NH_3 adsorption was carried out with 10% NH_3–N_2 gas mixture (25 ml min^{-1}) for 30 min at 50°C. The desorption was carried out from 50 to 550°C at 10°C min^{-1}. The TCD response was continuously monitored. For basicity measurements, an identical temperature, time, and flow profile were followed, except that a 10% CO_2–N_2 gas mixture was used as the treatment gas.

3. Results and discussion

3.1. Catalyst optimization

Five different V–Si–P catalysts were prepared with different ratios of the constituent atoms following the procedure outlined above. The activity of these catalysts was measured for the condensation reaction of PAA with formaldehyde and the most active catalyst was chosen for runs with PA and MP. Catalyst activity is defined as the yield of MAA based on PAA and formaldehyde fed to the reactor. The activity of five different V–Si–P catalysts for the condensation of formaldehyde with PAA is summarized in Table 2.

The most active catalyst (V–Si–P 1:10:2.8) was tested for condensation activity with PA and MP. The results, as summarized in Table 3, compare the condensation yield of these three propionates with formaldehyde at nominally identical operating conditions. This set of experiments shows that the yields (mole of MAA product/mole of HCHO charged and mole of propionate charged) are consistently higher for PAA and PA than those obtained for MP, indicating that while the acid and anhydride are relatively reactive, the ester propionate is difficult to condense [10].

The typical mechanism of condensation explains the difficulty of condensation for MP, whose α-hydro-

Table 2
Optimization of the V–Si–P ternary oxide catalyst [a]

Catalyst	Atomic ratio	Surface area(BET–N_2, $m^2\ g^{-1}$)	MAA yield [b]	MAA yield [c]
V–Si–P	1:12:2.8	96.5	52.7	22.6
V–Si–P	1:10:2.8	94.2	55.8	24.2
V–Si–P	1:2.8:2.8	24.5	38.4	16.5
V–Si–P	1:3.57:1	114.2	38.9	16.6
V–Si–P	1:10:10	3.24	9.46	4.06

[a] Reaction conditions: T=300°C; pressure=2 atm (30 psi in-house nitrogen), mole flow rates of propionic anhydride:for maldehyde:nitrogen=41:17:220 mmol h^{-1}.
[b] Yield based on charged HCHO.
[c] Yield based on charged PAA.

Table 3
Condensation of propionates with formaldehyde [a]

Type of propionyl	Space velocity (cc g^{-1} cat·h)	MAA yield (%, based on HCHO)	MAA yield (%, based on propionyl)
PAA [b]	290	76.8	36.4
PAA	480	36.4	16.7
PAA	900	30.1	14.7
PA [c]	320	60.5	12.9
PA	480	55.3	11.3
PA	900	45.8	9.82
MP [d]	320	22.2 [d]	4.83
MP	320	21.7	4.72
MP	900	9.61	2.08

[a] Reaction conditions: T=300°C; pressure=2 atm (30 psi in-house nitrogen).
[b] PAA=propionic anhydride; nominal mole flow rates of PAA : formaldehyde : nitrogen=41:17:220 mmol h^{-1}.
[c] PA=propionic acid; PA:formaldehyde:nitrogen=72:15.5:220 mmol h^{-1}.
[d] MP=methyl propionate; MP:formaldehyde:nitrogen=61:13.3:220 mmol h^{-1}; product contains both MMA and MAA; MMA/(MMA+MAA)=0.69.

gen is very difficult to abstract. The mechanism of condensation can be summarized as follows:

- *activation of the reactant by basic sites of the catalyst*

$$R{-}CH_2 - X + B \rightarrow R - {}^{-}CH - X + BH^{+} (B{=}O^{-} \text{ or } OH^{-},\ R{=}CH_3,\ X{=}COOCH_3) \quad (9)$$

- *activation of HCHO by acidic sites of the catalyst*

$$HCHO + H^{+} \rightarrow H_2C^{+}OH \quad (10)$$

- *reaction of two intermediate molecules to form an aldol followed by dehydration*

$$R - {}^{-}CH{-}X + H_2C^{+}OH \rightarrow H_2C(OH) - C(H)R{-}X \rightarrow H_2C{=}CR - X + H_2O \quad (11)$$

Conceptually, there are advantages to using the carboxylic acid anhydrides in the condensation reaction with formaldehyde to yield the corresponding α-,β-unsaturated acid anhydrides. For example, as stated earlier, the condensation of formaldehyde with a carboxylic acid (or an ester) generates 1 mol of water as shown in Eq. (12):

$$RCH_2COOR' + HCHO \rightarrow RC(=CH_2)COOR' + H_2O \quad (12)$$

The liberated water inhibits further reaction of formaldehyde and carboxylic acid and in the case of ester feedstocks, leads to the hydrolysis of ester. When the reaction is run using an acid anhydride, water is consumed in a subsequent reaction to form free acid with the overall condensation reaction represented by Eq. (13):

$$(RCH_2CO)_2O + HCHO \rightarrow RCH(=CH_2)COOH + RCH_2COOH \quad (13)$$

The product α-,β-unsaturated acid may then be separated from the free saturated acid. One further advantage of using the anhydride is that the saturated acid co-product in Eq. (13) may be used to regenerate the corresponding carboxylic acid anhydride by any of the several known processes [11,12]. One particularly useful approach for PAA is shown in Eq. (14).

$$CH_3CH_2COOH + CO + CH_2{=}CH_2 \rightarrow (CH_3CH_2CO)_2O \quad (14)$$

Unfortunately, as noted by Holmes [4], the reaction of anhydrides with aliphatic aldehydes (including formaldehyde) in the condensed phase generally does not lead to condensation but to the formation of 1,1-dicarboxylates according to Eq. (16):

$$(RCH_2CO)_2O + R'CHO \rightarrow (RCH_2CO)_2CHR' \quad (15)$$

As a consequence, the condensation of anhydride with aldehydes has seen limited application outside of the well-documented condensation of aromatic aldehydes (which do not form diesters readily) with formaldehyde, which is known as the Perkin reaction.

The catalysts which prevent the production of the diester, or operate on the diester to produce the corresponding α-,β-unsaturated acids, are thus suited for the condensation of anhydrides with aliphatic aldehydes. Despite these potential advantages, review of the literature shows only one reference to catalysts capable of this transformation [4]. The V–Si–P ternary catalysts are thus a novel class of catalysts capable of condensing a number of anhydrides into the corresponding α-, β-unsaturated acids.

3.2. *Measurement of acid–base properties*

The mechanism of condensation (Reactions (9)–(11)) clearly implies that both acid and base properties are needed for an active and selective catalyst, and that there may possibly be a correlation between the acid–base site distribution and the condensation yields [13]. This correlation was explored by measuring the acid–base properties of the catalysts tested for condensation reaction.

The acid–base property measurements were carried out on an ALTAMIRA catalyst characterization system. The results were quantified in terms of μmol probe (NH_3 and CO_2) adsorbed/g catalyst and m^2 surface area of the catalyst and are summarized in Table 4. The characteristic NH_3- and CO_2-temperature programmed desorption (TPD) patterns for each of the five catalysts above have been compared in Figs. 3 and 4, which give the NH_3–TPD patterns (measuring acidity) and the CO_2–TPD patterns (measuring basicity). The optimum V–Si–P 1:10:2.8 and 10% Ta-Nalco 1034A catalysts do not exhibit a prominent high temperature NH_3 and CO_2 desorption peak in the range of 573–823 K, while V–Si–P 1:2.8:2.8 and V–Si–P 1:10:10 show characteristic high temperature desorption peaks for both NH_3 and CO_2. The high temperature desorption peaks correspond to high strength acid and base sites. The presence of high temperature peaks, i.e., strongly acidic and basic sites, does not correspond to high condensation yields. This suggests that the strong acid and base sites may react irreversibly with the reactant molecules (PAA, PA and formaldehyde). Although the high temperature peak is also present in V–Si–P 2.8:10:2.8, the peak is clearly not as strong as that for V–Si–P 1:2.8:2.8 and 1:10:10. Further, the V–Si–P 2.8:10:2.8 catalyst also has a prominent acid–base peak in the medium temperature region corresponding to 423 to 573 K.

It is clear from the above discussion that the presence of high temperature peak ($573<T<823$ K) is detrimental to high condensation yields. The distribution of both acid and base sites as a function of temperature (i.e., as a function of strength) can be quantified by deconvoluting the TPD spectrum (NH_3–TPD pattern for distribution of acid sites as a function of temperature and CO_2–TPD pattern for the distribution of base sites as a function of temperature). The distribution of the catalyst sites of a particular type (acid or base), as a function of temperature range, can be quantified by a well-defined ratio of the following form [14]:

$$q = A(\text{desorbed from } 323 < T < 573\text{K})/A(\text{desorbed from 323K to 823K}) \quad (16)$$

where A (desorbed at 323 to 573 K), the denominator of Eq. (16), is the total area under the TPD spectrum. The results of the deconvoluted CO_2–TPD profiles in terms of the q-ratio have been summarized in Table 5.

The q-ratios for the V–Si–P series of catalysts (1:12:2.8, 1:10:2.8 and 1:3.57:1) are 0.388, 0.426 and 0.271, respectively. The q-ratio for the 10%

Table 4
Effect of catalyst acid–base properties on MAA yield [a]

Catalyst (atomic ratio)	Surface area (BET–N_2, $m^2\ g^{-1}$)	Total acidity (μmol $NH_3\ g^{-1}$ cat)	Total acidity (μmol $NH_3\ m^{-2}$ cat)	Total basicity (μmol $CO_2\ g^{-1}$ cat)	Total basicity (μmol $CO_2\ m^{-2}$)	MAA yield [b]	MAA yield [c]
V–Si–P (1:12:2.8)	96.5	155.7	1.62	100.2	1.04	52.7	22.6
V–Si–P (1:10:2.8)	94.2	150.8	1.61	96.5	1.01	55.8	24.2
V–Si–P (1:2.8:2.8)	24.5	124.5	5.11	99.8	4.07	38.4	16.5
V–Si–P (1:3.57:1)	114.2	174.9	1.53	59.1	0.52	38.9	16.6
V–Si–P (1:10:10)	3.24	81.8	25.2	74.0	22.8	9.46	4.06
Ta-1034A (10%)	132.1	24.52	0.186	26.0	0.197	46.4	19.9

[a] Reaction conditions: T=300°C; pressure=2 atm (30 psi in-house nitrogen), mole flow rates of propionic anhydride:formaldehyde:nitrogen=41:17:220 mmol h^{-1}.
[b] Yield based on charged HCHO, i.e., $\frac{\text{mole MAA}}{\text{mole charged HCHO}} \times 100$. Selectivity to MAA is typically >98%.
[c] Yield based on charged PAA.

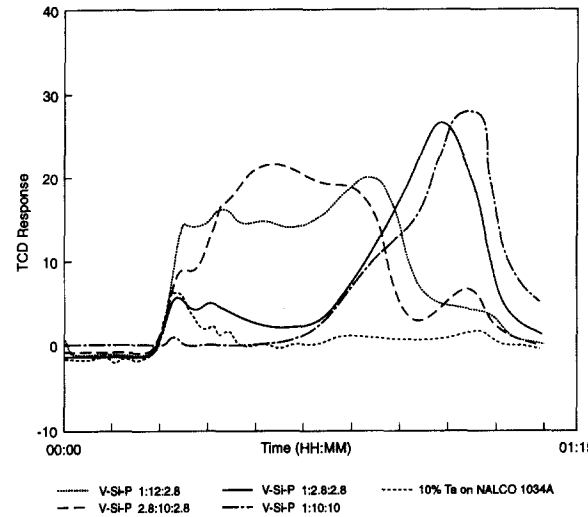

Fig. 3. NH_3–TPD spectra of V–Si–P and tantalum catalysts.

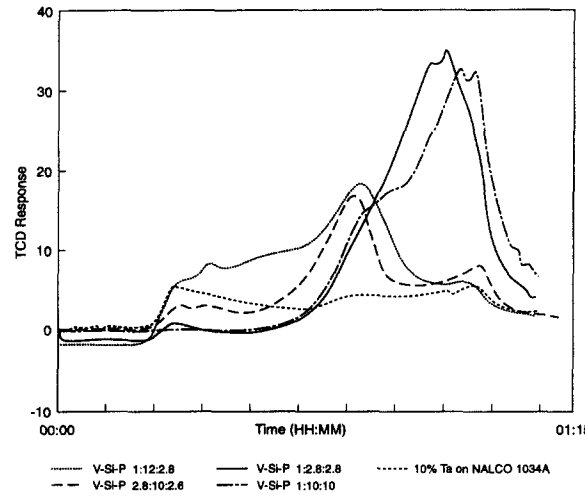

Fig. 4. CO_2–TPD spectra of V–Si–P and tantalum condensation catalysts.

Ta-NALCO SiO_2 catalyst is also high at 0.278. The catalysts with lower q-ratios have lower condensation yields, as evidenced by catalyst V–Si–P 1:10:10. The yield of the catalyst V–Si–P 1:2.8:2.8 is also high at 38.4%, although this catalyst has a characteristically low q-value of 0.086. The catalyst V–Si–P 1:10:10 which gave the lowest MAA yield has both a low q-ratio (of 0.063) and a very low surface area (3.24 $m^2\ g^{-1}$). Thus, there is a direct correlation between surface area, q-ratio and MAA yield.

Table 5
Deconvolution of CO_2–TPD profiles for condensation catalysts

Catalyst (atomic ratio)	Surface area (BET–N_2, $m^2\ g^{-1}$)	MAA yield [a]	q-ratio
V–Si–P (1:12:2.8)	96.5	52.7	0.388
V–Si–P (1:10:2.8)	94.2	55.8	0.428
V–Si–P (1:2.8:2.8)	24.5	38.4	0.086
V–Si–P (1:3.57:1)	114.2	38.9	0.271
V–Si–P (1:10:10)	3.24	9.46	0.063
10% Ta/SiO_2	132.1	46.4	0.278

[a] Yield based on charged HCHO, i.e., $\frac{\text{mole MAA}}{\text{mole charged HCHO}} \times 100$.

3.3. *Estimation of activation energy of the desorption peaks*

The activation energy of the desorption peaks gives a quantitative measure of the energy barriers to the desorption processes. The presence of the high temperature peak in both NH_3 and CO_2 desorption spectrum ($573<T<823$ K) corresponds directly to lower condensation yields. The strongly acidic sites, corresponding to high NH_3 desorption tempratures, may react irreversibly with the substrate molecules. A higher activation energy of the desorption peak will then represent an energy barrier which a substrate molecule must overcome to make it reactive.

The basic procedure for the determination of activation energy of desorption processes has been covered in detail in references [15,16]. For first-order desorption with a linear heating schedule, and in absence of any intra- and interparticle diffusional effects, the material balance of a sample presorbed on the solid adsorbent and then thermally desorbed into a carrier gas is given by:

$$-\nu_m(\delta\theta/\delta t) = \nu_m k_d\theta - k_a C(1-\theta) \tag{17}$$

and

$$FC = V_s\nu_m k_d\theta - V_s k_a C(1-\theta) \tag{18}$$

In these expressions, ν_m represents the amount of sample adsorbed per unit volume of the solid phase when the surface coverage θ is unity, k_d and k_a are the rate constants of desorption and adsorption, respectively, C is the concentration of the sample in carrier gas, F is the carrier gas flow rate and V_s is the volume of the solid phase. For a linear heating schedule defined by:

$$T = T_0 + \beta t \tag{19}$$

and under the assumption that readsorption during the course of the TPD is negligible, the rate of desorption k_d can be related to the activation energy of desorption by:

$$(k_d)_M = A\exp(-E_d/RT_M) = \beta E_d/RT_M^2 \tag{20}$$

At any known rate of catalyst heating β, Eq. (20) defines the activation energy of desorption E_d for an observed temperature of peak maximum T_M. Given that A is known, or a reasonable value can be assumed for it, the value of E_d can be determined from Eq. (20).

Frequently, when 'A' values are not known or cannot be assumed within a reasonable range, Eq. (20) can be rewritten in the form:

$$2\ln T_M - \ln\beta = E_d/RT_M + \ln(E_d/AR) \tag{21}$$

Thus, a plot of $(2\ln T_M - \ln\beta)$ vs. $1/T_M$ will be, in principle, useful for determining E_d and A.

The V–Si–P series of catalysts were subjected to different desorption heating rates. Following isothermal adsorption from a 10% NH_3/N_2 adsorbing gas at 323 K for 30 min, the NH_3–TPD was carried out at five different heating rates, namely 1, 5, 10, 20, and 30°C min^{-1}. The characteristic NH_3–TPD curves for these five heating rates are shown in Figs. 5–9. The temperature of the peak maximum (for the high strength acid peak) as a function of the heating rate is summarized in Table 6.

The slope of the plot of $2(\ln T_M - \ln\beta)$ vs. $1/T_M$ is 1.28×10^4 K. The slope is the value of E_d/R, so the activation energy of the high temperature desorption peak is estimated to be 25.4 kcal mol^{-1}. It is clear from the MAA yield that the high temperature peak, corresponding to high strength acid sites, contributes directly to lower yields; thus, the activation energy of 25.4 kcal mol^{-1} represents an activity threshold. Cat-

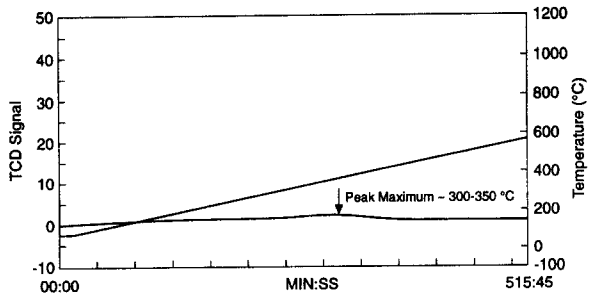

Fig. 5. NH_3–TPD pattern for V–Si–P 1:12:2.8 catalyst, TPD heating rate 1°C min^{-1}.

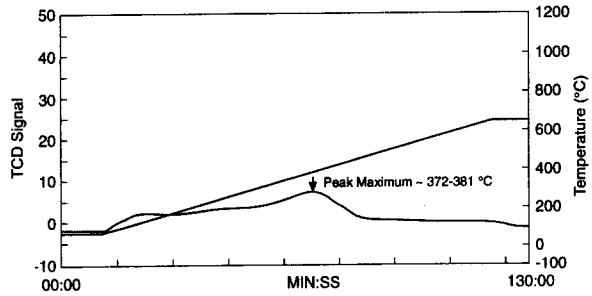

Fig. 6. NH_3–TPD pattern for V–Si–P 1:12:2.8 catalyst, TPD heating rate 5°C min^{-1}.

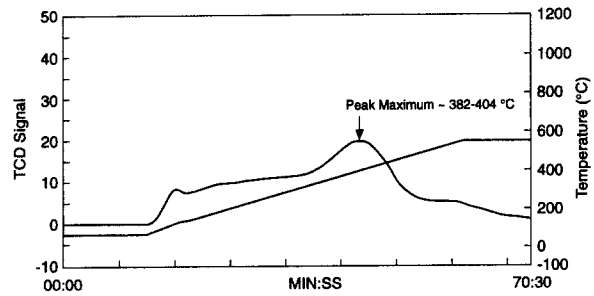

Fig. 7. NH_3–TPD pattern for V–Si–P 1:12:2.8 catalyst, TPD heating rate 10°C min^{-1}.

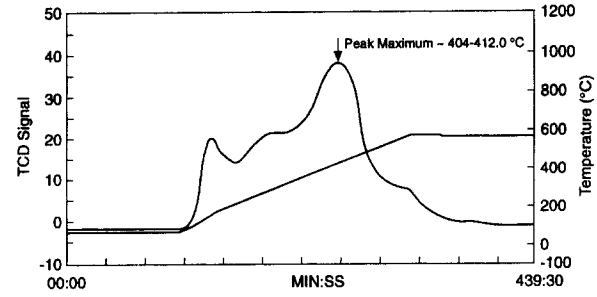

Fig. 8. NH_3–TPD pattern for V–Si–P 1:12:2.8 catalyst, TPD heating rate 20°C min^{-1}.

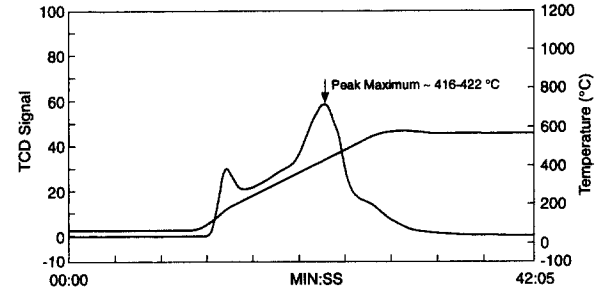

Fig. 9. NH_3–TPD pattern for V–Si–P 1:12:2.8 catalyst, TPD heating rate 30°C min^{-1}.

alysts exhibiting desorption peaks of activation energies $\geq$25.4 kcal mol^{-1} will be less active than the optimum V–Si–P catalyst. Further characterization of these high strength acid and base sites by substrate adsorption and desorption (including PAA and PA) is under way.

3.4. *Long-term activity check on V–Si–P 1:12:2.8 and Ta/1034A catalysts*

To investigate the long-term activity of the V–Si–P 1:12:2.8 and Ta/1034A catalyst, an extended run was

Table 6
Location of T_M as a function of β-high temperature peak

Heating rate β (°C min^{-1})	Range of T_M (K)	T_M (K)	$1/T_M$ ($\times 10^3$)
1	573–623	598	1.672
5	645–654	650	1.538
10	655–677	666	1.501
30	689–695	692	1.445

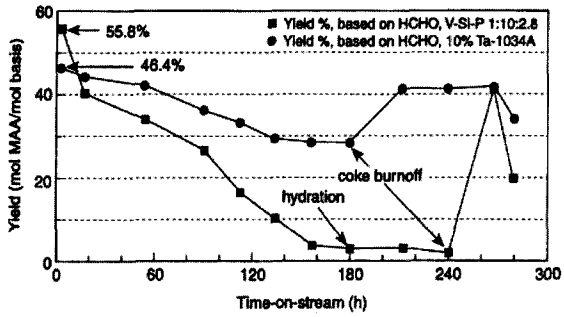

Fig. 10. Long-term deactivation pattern of V–Si–P and Ta catalysts. Experimental conditions: catalyst charge, 15 g; T=300°C; pressure=2 atm; feed, 41:17:220 mmol h^{-1} PAA:HCHO:nitrogen.

carried out with both catalysts. The initial MAA yield (based on charged HCHO) is higher for the V–Si–P catalyst, at 56%, compared to the 10% Ta/1034A catalyst is at 46.4%. However, after a 180 h period, catalyst activity drops significantly for both catalysts. For the V–Si–P catalyst, the MAA yield at t=4 h was 55.8% (based on charged formaldehyde), but dropped to 2.74% after 180 h (based on charged HCHO). This represented a drop in catalyst activity by nearly a factor of 20. The drop in catalytic activity for the 10% Ta/1034A is not as sharp; however, the activity drops from an initial value of 46.4% to 28% and is stable at 28% for nearly 54 h (Fig. 10). The causes of catalyst deactivation can be hypothesized to be:

- loss of acidity by hydroxyl groups;
- loss of surface area and/or porosity; and
- carbon deposition due to coking.

These causes have been investigated as follows:

3.4.1. *Catalyst hydration*

If the loss in catalyst activity was construed to be due to the loss in surface acidity, hydration of the catalyst may restore the surface hydroxyl groups. The deactivated catalyst was steam-treated under an inert nitrogen atmosphere for 24 h. Water was injected through a syringe pump at a nominal flow rate of approx. 300 mmol h^{-1}. Nitrogen was used as an inert diluent at 600 mmol h^{-1}. The concentration of steam was thus at 33.3% by volume. The catalyst activity was checked after a 24 h hydration of the catalyst. The results indicate that catalyst hydration is ineffective in restoring the catalyst activity. Fig. 10 shows this result for the V–Si–P catalyst. This also suggests that the loss in catalyst activity may not be due to loss of surface hydroxyl groups.

3.4.2. *Regeneration by flowing air oxidation at 300°C*

Since the catalyst activity could not be restored by hydration, coke formation was considered to be a more plausible reason for deactivation. The deactivated catalyst was treated at 300°C under a flowing air atmosphere (approx. 220 mmol h^{-1} for 24 h). The MAA yield (based on charged HCHO) was restored to 40.8%. When compared to the original MAA yield of 55.8% (based on charged HCHO), the oxidative regeneration restored about 78% of the original activity of the V–Si–P catalyst. For the 10% Ta/1034A catalyst, the regeneration restored the MAA yield from 28% to about 41.1%. When compared to original catalyst activity of 46.4%, the restored activity was about 88% of the original. However, the deactivation pattern continues after the oxidation regeneration for both V–Si–P and Ta catalysts (Fig. 10). The Ta catalyst is more stable and has a higher on-stream life, based on these catalyst long-term activity studies.

3.5. *Further studies on acid–base properties*

The effects of pretreatment time, temperature, and the acid–base properties of fresh and deactivated catalysts were studied with the goal of improving the overall catalyst on-stream life. The results have been summarized in Figs. 11–14. Fig. 11 shows the effect of pretreatment temperature of the surface acidity, while Figs. 12 and 13 show the effects of pretreatment time and deactivation on the surface acidity. Fig. 14 shows a comparative NH_3-TPD pattern for a fresh catalyst pretreated at 600°C for 6 h and a deactivated catalyst (180 h at 300°C and 2 atm, with mole flow rates of PAA:formaldehyde:nitrogen=41:17:220 mmol h^{-1}).

The results of TPD at pretreatment temperature of 300 and 600°C for an hour are shown together in Fig. 11. No apparent difference is observed between 300 and 600°C. This implies that the surface acidity is relatively insensitive to the pretreatment temperature between 300 and 600°C. This can further mean that the catalyst calcination temperature within this range may not affect the surface character, albeit the effect of

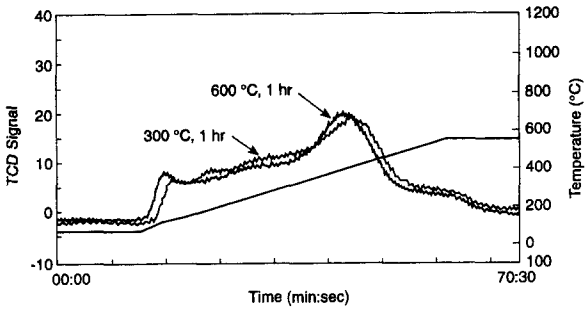

Fig. 11. NH_3–TPD pattern (surface acidity) of a V–Si–P 1:10:2.8 catalyst as a function of pretreatment temperature.

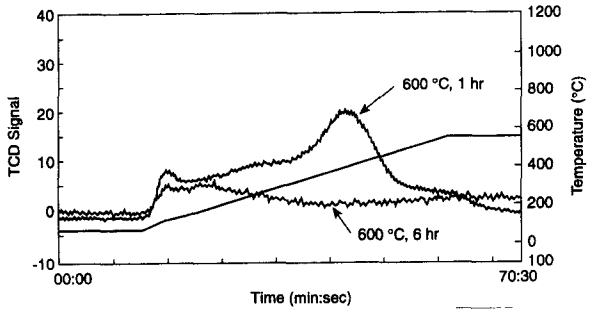

Fig. 12. NH_3–TPD pattern (surface acidity) of a V–Si–P 1:10:2.8 catalyst as a function of pretreatment time.

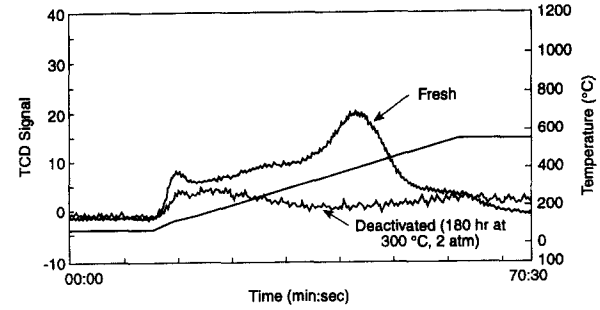

Fig. 13. NH_3–TPD pattern (surface acidity) of fresh and deactivated V–Si–P 1:10:2.8 catalysts.

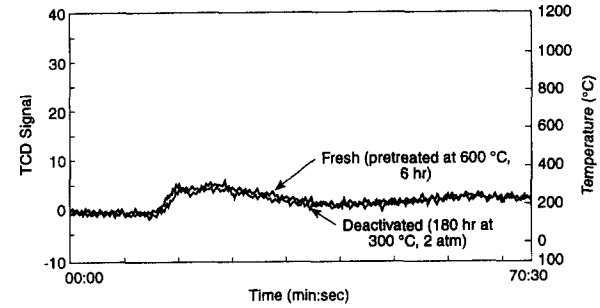

Fig. 14. Comparative NH_3–TPD patterns (surface acidity) of fresh and deactivated V–Si–P 1:10:2.8 catalysts.

calcination temperature on bulk surface area has not been studied. However, the length of time of pretreatment at 600°C showed a large effect on the total acidity and acid distribution. As shown in Fig. 12, the total acidity decreases about 80% (from approx. 150 μmol g^{-1} catalyst to approx. 30 μmol NH_3/g catalyst) and this decrease is mainly attributable to the high temperature peak (T>300°C), namely, strong acidic sites. It is clear that a longer heat treatment destroys these stronger acid sites preferentially; however, the mechanism of this preferential destruction is an open question.

Fig. 13 compares the TPD results of the fresh and deactivated catalysts. The fresh catalyst in this case was pretreated at 600°C for 1 h, although, as evidenced in Fig. 11, the pretreatment temperature does not affect the surface features. The results demonstrate that 180 h on stream at 300°C and 2 atm, with the inlet mole ratios of PAA:formaldehyde:nitrogen=41:17:200 mmol h^{-1}, decreases the total acidity and changes the acid site distribution dramatically. Again, the strong acid sites are preferentially destroyed. This suggests that catalyst deactivation is caused by coking of the strong acidic sites. In addition, the similarity between the loss of strong surface acidity of the deactivated V–Si–P catalyst, and this same fresh catalyst pretreated at 600°C for 6 h in the absence of reactants that could form coke (Fig. 14), suggests that the catalyst may deactivate due to thermal effects alone. Although the deactivated V–Si–P catalyst was exposed to only 300°C, compared to 600°C for the fresh catalyst, the deactivated catalyst was on-stream for a substantial longer time (180 h)than the 6 h for which the fresh catalyst was pretreated. Thermal effects alone may thus account for the observed loss of acid sites on both catalysts.

Based on the acid–base property study, a low surface acidity with a high q-ratio coupled with an effective reactor heat removal scheme would be needed for a commercial condensation catalyst. The use of slurry reactors for condensation of PAA with

formaldehyde to produce MMA is currently being studied in our laboratories. Key issues regarding the choice of slurry fluids, gas solubility and vapor liquid equilibrium measurements, and thermal stability are also being resolved.

4. Conclusion

In summary, we conclude that the V–Si–P ternary catalyst and Ta-silica catalysts are active and selective for the condensation of PAA with formaldehyde. Catalysts that exhibit higher condensation yields have a characteristic low temperature acid and base desorption peaks in the temperature range of 323–573 K and an absence of high temperature peak in the range of 573–823 K. A parameter called the q-ratio is also defined which is measure of the distribution of acid or base sites as a function of temperature. A higher value of q-ratio is desirable for improved catalyst performance along with a high surface area. The activation energy of the high strength acid sites is estimated to be 25.4 kcal mol^{-1}. The estimations of acid–base correlations and activation energies will be used to 'design' a second generation of more active and stable condensation catalysts. [14]

References

[1] M. Ai, J. Catal., 107 (1987) 201.
[2] M. Ai, J. Catal., 124 (1990) 293.
[3] M. Ai, Appl. Catal., 63 (1990) 29.
[4] J.D. Homes, U.S. Patent No. 4 085 143 (1978).
[5] J.J. Spivey, M.R. Gogate, B.W.L. Jang, E.D. Middlemas, J.R. Zoeller, S.S. Tam and G.N. Choi, in Proceedings of the Contractor's Review Meeting on Coal Liquefaction and Gas Conversion, USDOE/PETC, Pittsburgh, PA, 1995, pp. 385–395..
[6] J.J. Spivey, M.R. Gogate, E.D. Middlemas, J.R. Zoeller, S.S. Tam, and G.N. Choi, Invited Paper Presented at the Second World Environmental Congress, London, Ontario, September 11–16, 1995..
[7] J.J. McKetta (Ed.), Encyclopedia of Chemical Processing and Design, Vol. 30, 1989..
[8] O.H. Bailey, R.A. Montag and J.S. Yoo, Appl. Catal. A: General, 88 (1990) 163.
[9] J.S. Yoo, Appl. Catal. A: General, 102 (1993) 215.
[10] M.R. Gogate, J.J. Spivey and J.R. Zoeller, in Proceedings of the ACS National Meeting, Division of Petroleum Chemistry, Symposium of Syngas Conversion to High Value Chemicals, New Orleans, LA, 1996 pp. 216–219..
[11] S.L. Cook, Acetic Anhydride, in V.H. Agreda and J.R. Zoeller (Eds.), Acetic acid and its derivatives, chapter 9, Marcel Dekker, New York, NY, 1993..
[12] W. Reppe and W. Schweckendiek, U.S. Patent No. 2 658 075, 1953; W.F. Gresham and R.E. Brooks, U.S. Patent No. 2 497 304, 1950; D. Forster and A. Hershman, U.S. Patent No. 3 989 751, 1976; N. Rizkalla, U.S. Patent No. 4 483 803, 1984..
[13] J.J. Spivey, M.R. Gogate and J.R. Zoeller, in Proceedings of the ACS National Meeting, Division of Petroleum Chemistry, Symposium of Syngas Conversion to High Value Chemicals, New Orleans, LA, 1996, pp. 233–237..
[14] T. Kanno and M. Kobayashi, in H. Hattori, M. Misono and Y. Ono (Eds.), Acid–Base Catalysis II, chapter 2.14, Elsevier, Tokyo, 1994..
[15] R.J. Cvetanovic and Y. Amenomiya, Catal. Rev., 6 (1972) 21.
[16] Y. Amenomiya, CHEMTECH, 2 (1976) 128.